Journal of Microscopy, Vol. 232, Pt 1 2008, pp. 158–163
Received 24 January 2008; accepted 20 March 2008

Second-harmonic microscopy of *ex vivo* porcine corneas

B. VOHNSEN*† & P. ARTAL*
*LOUM, CIOyN, Murcia University, 30071 Murcia, Spain
†School of Physics, University College Dublin, Belfield, Dublin 4, Ireland

Key words. Collagen fibrilis, cornea, nonlinear optics, second harmonic.

Summary

The *ex vivo* cornea of porcine eyes has been studied with second-harmonic microscopy with a laboratory-built system to examine the structure of collagen fibrils at different length scales, as well as the image dependence on polarization and wavelength of the illumination source. We found that collagen fibrils can effectively be visualized with second-harmonic microscopy, in agreement with previous findings, at different wavelengths of the illumination. The same laser source used for imaging may also be used to induce changes to the corneal tissues that are observable both in the linear and second-harmonic imaging channels. Such studies are essential first steps towards a future high-resolution optical characterization technique for simultaneous corneal surgery and wound healing of the human eye.

Introduction

Recent years have witnessed major advances in multiphoton techniques with a wealth of novel high-resolution imaging modalities that have confirmed great potential in the bio- (Zipfel *et al.*, 2003) and material sciences (Labarthet & Shen, 2003). For biological samples, two-photon fluorescence microscopy has become a well-established technique that allows for large penetration depths (∼mm) and a minimum of light-induced damage as the interaction is essentially confined by the focal volume. Likewise, second-harmonic (SH) generation microscopy has shown great potential in the imaging of photonic materials down to a nanoscale (Vohnsen & Bozhevolnyi, 2001; Vohnsen *et al.*, 2001; Labarthet & Shen, 2003; Zayats & Smolyaninov, 2004), to reveal local symmetries in biological samples (Moreaux *et al.*, 2000), visualization of muscle tissues (Freund & Deutsch, 1986; Chu *et al.*, 2003) and the fibril organization in collagen-rich tissues such as skin (Palero *et al.*, 2006), the cornea and the sclera of the eye (Hochheimer, 1982; Yeh *et al.*, 2002; Han *et al.*, 2004; Han *et al.*, 2005; Tan *et al.*, 2005; Teng *et al.*, 2006; Morishige *et al.*, 2007; Svoboda *et al.*, 2007; Vohnsen & Artal, 2007). Likewise, SH imaging has been successfully used to image the *ex vivo* optic nerve head (Brown *et al.*, 2007) with important implications for glaucoma analysis. Eventually, the combination of multiphoton microscopy with adaptive optics (Vargas-Martín *et al.*, 1998; Fernández *et al.*, 2001) could permit to increase the range of imaging possibilities, including the living eye and retina (Hermann *et al.*, 2004; Vohnsen *et al.*, 2005a).

The ordered structures of collagen fibrils, that are known to form the backbone of the cornea, are responsible for its mechanical properties (Boote *et al.*, 2003) as well as its optical properties such as birefringence, scattering and transparency to visible light (Smith, 2007). The collagen fibrils have traditionally been analysed with electron and scanning probe microscopy. However, the elongated structure of individual collagen-I molecules are known to be efficient converters of incident light to SH radiation, with an effective nonlinear susceptibility on the order of ∼0.4 pm/V or more (an estimation based on rat-tail tendon; Stoller *et al.*, 2003). This has been explored in recent studies by imaging post-mortem the structure of collagen fibrils both in animal and human corneas. The true interest of SH imaging for the cornea is eventually to allow *in vivo* imaging of the fibrils during and following corneal surgery taking advantage of the fact that no dyes are required in the process. In one notable case, intrastromal nanosurgery combined with multiphoton imaging has already been accomplished with *in vivo* anaesthetized rabbits (Wang & Halbhuber, 2006).

In this work, we present results obtained with a laboratory-built scanning optical microscope confirming previous reports on the ordered collagen fibril structures (Hochheimer, 1982; Yeh *et al.*, 2002; Han *et al.*, 2004, 2005; Tan *et al.*, 2005; Teng *et al.*, 2006; Morishige *et al.*, 2007; Svoboda *et al.*, 2007; Vohnsen & Artal, 2007). The dependence on polarization and spectrum is explored, and finally also light-induced thermal changes are examined as a precursor to future work directed towards corneal surgery of the human cornea.

Experimental system

For the reported nonlinear susceptibility (Stoller *et al.*, 2003), first harmonic (FH), i.e. the directly transmitted light, and SH

Correspondence to: Brian Vohnsen. Tel: (+353) 1-716-2217; fax: (+353) 1-283-7275; e-mail: brian.vohnsen@ucd.ie

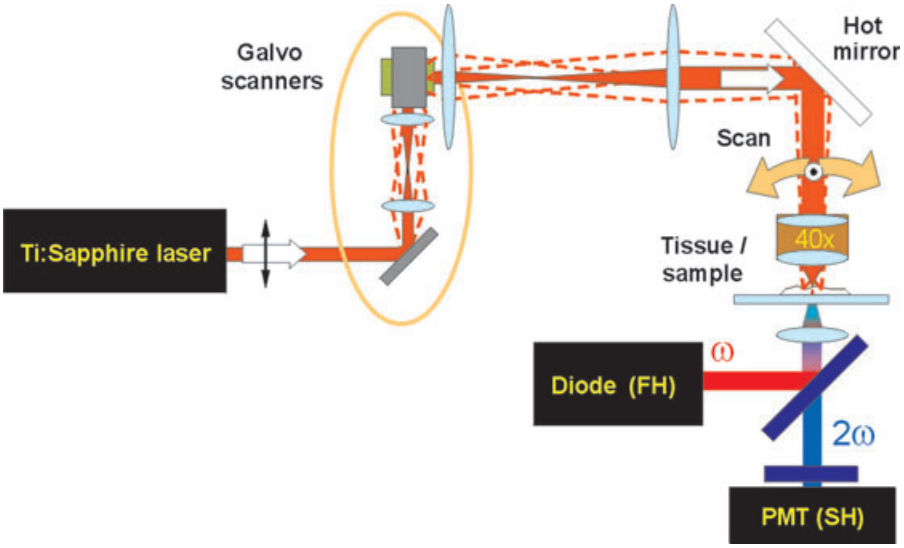

Fig. 1. Schematic of the second-harmonic microscope system used (optional λ/2 plate not shown). The FH (ω) and SH (2ω) signal channels are both indicated.

signals would be comparable at intensities on the order of $\sim 10^{17}$ W cm^{-2} (or equivalently a tightly focused peak power on the order of ~1 GW) and thus showing the need of an ultra-short-pulsed illumination source. Here a tunable Ti:Sapphire laser system (Coherent Mira, Santa Clara, CA, USA) emitting pulses of ~110 fs at 76 MHz is used in an in-house built microscope system. The scanning is realized by use of two non-resonant galvanometric scanners in conjugate planes that sweep a focused beam across the tissue being imaged. In the results presented, typically an average power in the range of 50–100 mW is incident onto the tissue corresponding to peak powers of ~5–10 kW. The transmitted light collected with a low numerical aperture (NA) lens (~0.40) is measured with a photodiode at the fundamental frequency whereas a set of filters is used together with a photomultiplier tube (Hamamatsu R7205-01, Hamamatsu, Shizuoka, Japan) and a photon counting unit (Hamamatsu C6465) to isolate the frequency-doubled signal relevant for collagen detection. The photon counting gate is set to a maximum of 12.75 μs/pixel (i.e., ~1000 pulses from the Ti:Sapphire laser) with typical count rates on the order of 100 photons/pixel. Total imaging speed is adjustable but is typically set at a frame rate of one image per minute for 100 × 100 image pixels (the speed is currently limited by the use of non-resonant scanners). Two different long-working-distance microscope objectives have been used: magnification ×40 (NA = 0.60) and ×100 (NA = 0.80) both without immersion as opposed to most of other reported studies (Han *et al.*, 2004, 2005; Tan *et al.*, 2005; Teng *et al.*, 2006; Morishige *et al.*, 2007) as this makes the situation more similar to a possible realization in the living eye. The small difference in NA of the objectives gains in importance for nonlinear imaging in providing almost two times higher transverse resolution and four times higher depth selectivity (scaling as NA^2 and NA^4, respectively). For both objectives the entrance pupil has been overfilled to guarantee full usage of their respective NA. The calibration of the system has been presented elsewhere (Vohnsen & Artal, 2007). A schematic diagram of the system is shown in Fig. 1.

The present system operates in transmission, but the indicated hot mirror ensures that it can easily be reconfigured to operate in reflection mode as would eventually be required for whole eye (and *in vivo*) studies. Typically, the coherent scattering in the SH process from the cornea collagen fibrils makes the signal strongest in the forward direction [although typically recognizable in the backward direction too (Morishige *et al.*, 2007)], whereas in the sclera a similar strong SH reflection has been reported (Yeh *et al.*, 2002).

The corneal tissues were obtained from porcine eyes obtained within a few hours from slaughter. They were cut in the laboratory with an 8.25 mm trephine just before imaging. The isolated corneas were washed and wedded with phosphate-buffered saline and mounted on microscope slides with a thin cover glass (~0.15 mm) to reduce evaporation and to improve on the optical quality.

Experimental results and discussion

The simultaneous measurement of FH and SH provides complimentary insight and the photon counting can also provide additional details such as, e.g. the standard deviation measured at each point, an example of which is shown in Fig. 2. Clearly, no fibril structure is observable in the FH image but in turn it is clearly visible in the SH image confirming the suitability of SH as the chosen imaging technique. The

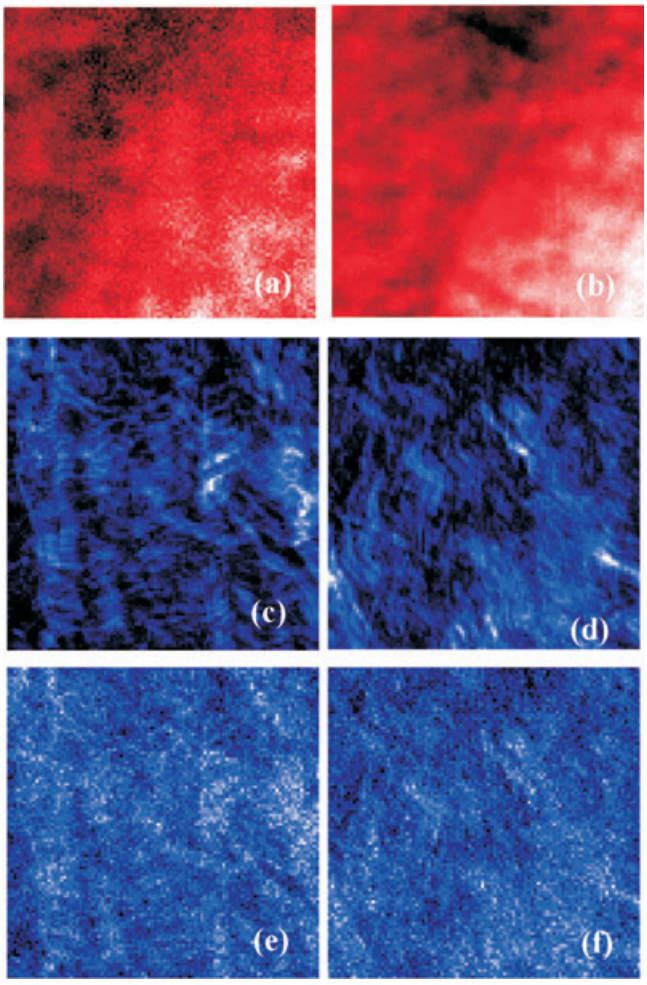

Fig. 2. Output signal channels in the microscope include (a, b) first harmonic (FH), (c, d) second harmonic and (e, f) standard deviation of photon count (approximately equal to the square root of the second harmonic signal). Left column (a, c, e) recorded near the corneal surface, right column (b, d, f) recorded at 50 μm depth. All images are approximately 60 × 60 μm^2 and have been obtained with a ×40 microscope objective and vertical orientation of the incident linearly polarized illumination. The RMS contrasts of the normalized images are (a) 0.17, (b) 0.19, (c) 0.14, (d) 0.15, (e) 0.14 and (f) 0.14. The colour scale [black, red, white] represents FH and [black, blue, white] represents second-harmonic signals in this and the following figures.

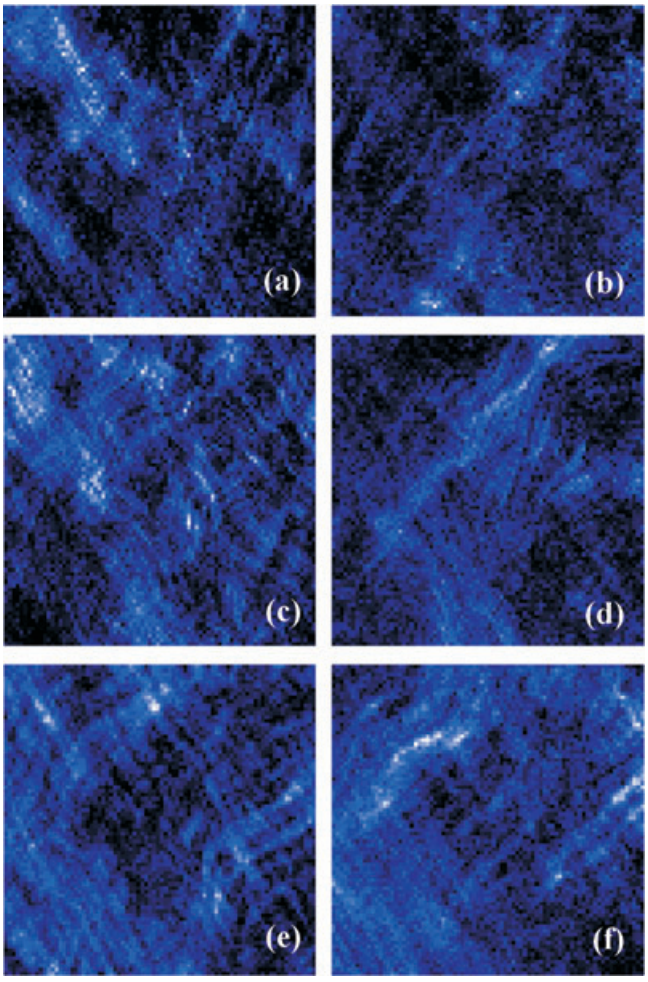

Fig. 3. Second-harmonic images obtained at different scales and with orthogonal linear polarizations [vertical in the left column (a, c, e) and horizontal in the right column (b, d, f)] of the incident light. Image size is (a, d) 100 × 100 μm^2, (b, e) 50 × 50 μm^2 and (c, f) 25 × 25 μm^2; each set is an experimental zoom-in on the central part of the larger image. All images have been obtained with a ×100 microscope objective. The RMS contrasts of the normalized images are (a) 0.14, (b) 0.11, (c) 0.15, (d) 0.11, (e) 0.13 and (f) 0.14.

standard deviation images (obtained from a set of 100 repeated photon count measures at each pixel) resemble the SH images although the contrast is less marked as to be expected from Poisson statistics of the photon count numbers (Qu & Singh, 1995). The statistics of the SH photon count gives additional insight and may be of value for posterior image processing. It is possible to quantify the image contrast in terms of a global root-mean-square (RMS) contrast for each image (Bueno & Vohnsen, 2005). All images (Fig. 5 apart) have been obtained with a central wavelength of 800 nm of the fundamental FH illumination.

The polarization of the incident light is an important parameter that may be varied to highlight any given orientation of fibrils (Palero *et al.*, 2006). We have used a λ/2 wave plate (not shown in Fig. 1) to switch between orthogonal orientations of the incident linearly polarized light beam and have done imaging at different scales as shown in Fig. 3. Clearly, the choice of polarization may serve to highlight different orientations of collagen fibrils in agreement with earlier findings (Yeh *et al.*, 2002) although the relation is not trivial. It is to be expected that analysing the polarization at the detector can provide additional insight although at the cost of signal (Vohnsen & Bozhevolnyi, 2001; Bueno & Vohnsen, 2005). Note that the higher NA of the microscope objective used for these images allows higher-resolution imaging that

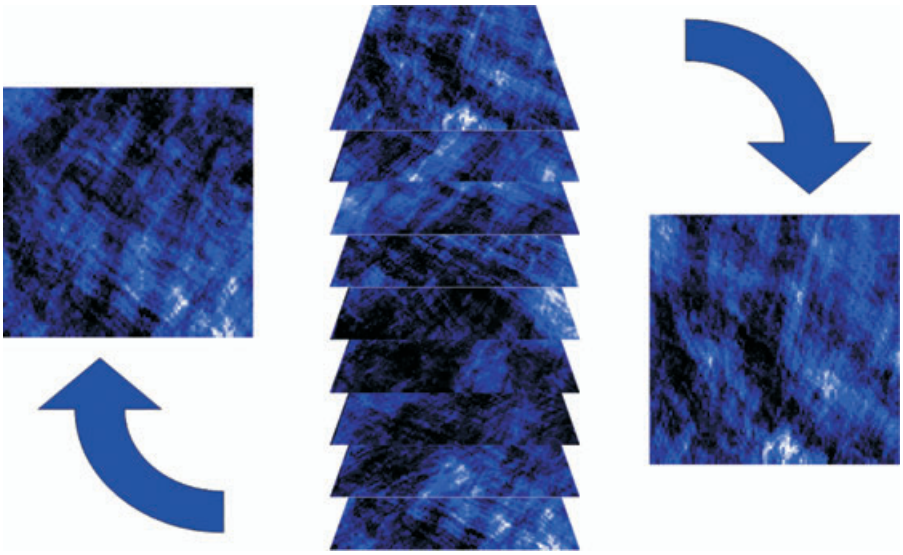

Fig. 4. Stack of 60 × 60 μm^2 second-harmonic images recorded at different depths of the stroma (total vertical range of 200 μm) from deep within (left) to near Bowman's layer (right) with a ×40 microscope objective.

better reveals the wavy structure of the cross-hatched network of fibril bands.

When imaged in depth the variation in collagen distribution becomes apparent as shown in Fig. 4. For instance, it has recently been shown that inclined elongated collagen fibrils of ∼120-μm length are present up to the Bowman layer in the human cornea (Morishige *et al.*, 2007). Although most imaging is done at or near an excitation wavelength of 800 nm we show in Fig. 5 that this is not a strict condition as indeed imaging at other wavelengths can also provide high-quality imaging of the collagen fibrils. These images were recorded in a time interval of about 5 min and clearly some drift is visible on the FH images (evidenced by the trapped air that gradually shifts downwards).

With only small modifications the same system used for the imaging may also be used to introduce changes to the corneal structure at different scales as shown in Fig. 6. Such studies are relevant in that they may open up for future *in vivo* studies that combine corneal surgery with an imaging technique capable of showing changes induced to the collagen fibril distribution *in situ* or immediately after surgery (Wang & Halbhuber, 2006). Here, the change is caused by local heating of the cornea and this gives rise to a nontrivial behaviour and eventually a decay of the SH signal measured during light exposure for a fixed cornea position. Similar enhancements of SH signal have recently been observed for human keratoconus corneas as a result of a piling up of collagen fibrils (Morishige *et al.*, 2007). The nontrivial variation in SH signal as a function of time during the exposure reflects a dependence on temperature of the strength of the SH radiation (Tan *et al.*, 2005), although in the present case the modification is highly localized. Indeed, localized bubbles may form once the threshold for plasma formation has been surpassed (Sun *et al.*, 2007). The corresponding FH images show clearly a marked drop in transparency of the tissue once the light-induced feature is large. In consequence, simultaneous observation of FH and SH images is important in order to exclude possible variations in the nonlinear image caused by linear (absorption, scattering) properties only. Even longer exposures were also tried but these lead to dramatic changes on a much larger scale due to evaporation.

Conclusions

Although the present work like most other studies (Hochheimer, 1982; Yeh *et al.*, 2002; Han *et al.*, 2004, 2005; Tan *et al.*, 2005; Teng *et al.*, 2006; Morishige *et al.*, 2007; Sun *et al.*, 2007) only examine post-mortem ocular tissues, SH microscopy does hold promise for future *in vivo* applications with larger signals as obtainable with shorter laser pulses and correspondingly higher peak powers than currently used. If accomplished, such studies are bound to be performed in reflection or backscattered configurations but this is also practically realizable as the strength of the SH signal and image quality in such a configuration can be similar (Han *et al.*, 2005; Tan *et al.*, 2005; Teng *et al.*, 2006; Morishige *et al.*, 2007). We have found that nonlinear imaging is an attractive alternative to more conventional imaging modalities that may in the near future be further explored in real-life applications such as real-time monitoring of change induced during corneal surgery of the human eye. The combination with other imaging modalities (including FH and eventually also multiphoton fluorescence) can enrich the palette of information obtainable simultaneously through imaging. The intrinsic dependence of

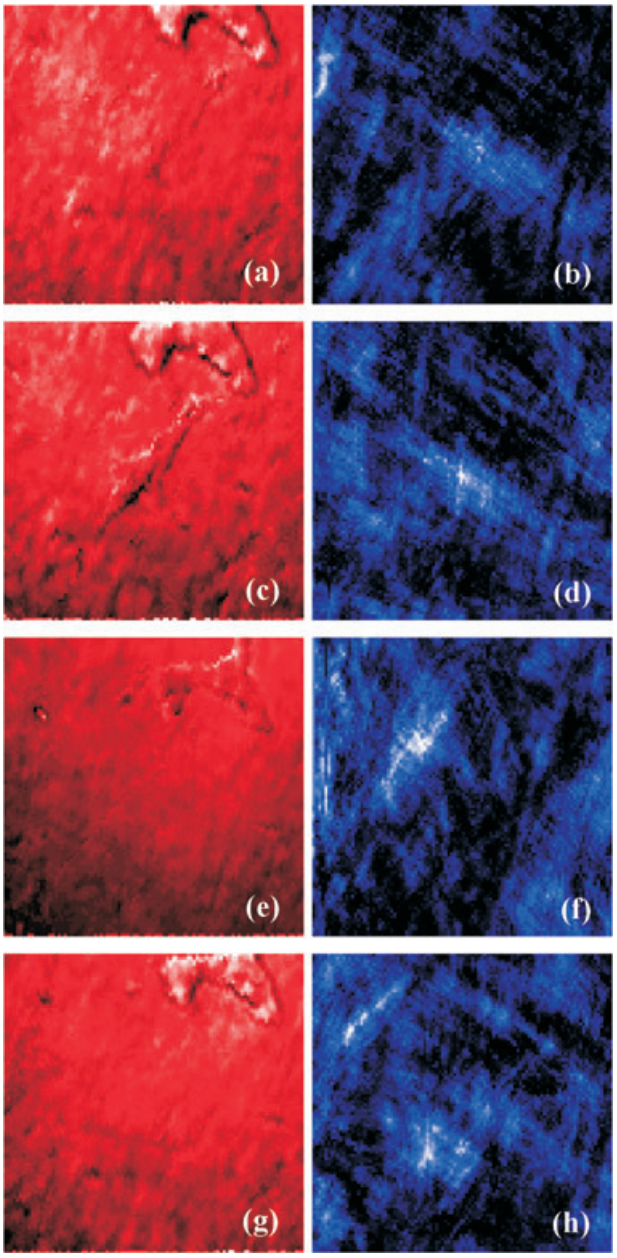

Fig. 5. Variation of first and second-harmonic images obtained with different central wavelengths of the incident illumination: (a, b) 750 nm, (c, d) 800 nm, (e, f) 850 nm and (g, h) 900 nm. All obtained with a ×40 microscope objective. Images (a, b) were recorded first and (e, f) were recorded last showing a noticeable drift downwards during imaging. Incident light is vertically polarized. All images are 125×125 μm^2 and have been obtained with a ×40 microscope objective.

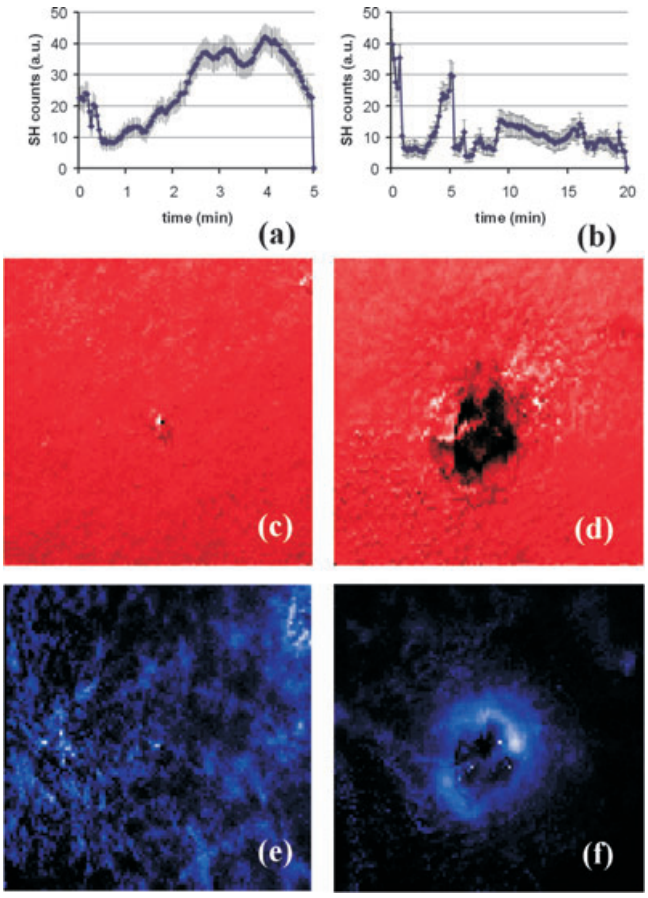

Fig. 6. Light-induced changes to the corneal tissue at a (a, c, e) small and (b, d, f) large scale: (a, b) second-harmonic signal variation versus time recorded during exposure at a fixed position for 5 and 20 min, respectively (±SD shown), (c, d) first-harmonic images recorded immediately after ended exposure and (e, f) simultaneously recorded second-harmonic images. Image size is 125×125 μm^2 and the results have been obtained with a ×40 microscope objective.

the SH signal on the details of the collagen fibrils provides important complementary insight into the structure and properties of the cornea. Eventually, similar studies may be applied at the level of the retina in order to gain insight into its optical properties and improve the understanding of its interaction with light (Vohnsen *et al.*, 2005b; Franze *et al.*, 2007; Vohnsen & Artal, 2007). The future combination of this type of multiphoton microscopy with adaptive optics would permit us to follow changes in corneal properties at different depths after ablation of tissue. This could be an important addition among improved techniques of corneal refractive surgery, providing patients with a better post-surgery optical quality.

Acknowledgements

We wish to acknowledge the help of C. Molero and J. M. Marín from Hospital Virgen de la Arrixaca, Murcia for help with cornea preparations, M.C. Ortíz at Universidad de Murcia for proving us with phosphate-buffered saline, and Ganados Rio Segura who kindly provided the porcine eyes used in this study. The research has been realized with financial support from the Ministerio de Educación y Ciencia (Spain)

(grants FIS2004-02153, FIS2007-64765 and RYC2002-006337) and Fundación Seneca (grants 03115/PI/05 and 4524/GERM/06).

References

Boote, C., Dennis, S. Dennis, Newton, R.H., Puri, H. & Meek, K.M. (2003) Collagen fibrils appear more closely packed in the prepupillary cornea: optical and biomechanical implications. *Inv. Ophthalmol. Vis. Sci.* **44**, 2941–2948.

Brown, D.J., Morishige, N., Neekhra, A., Minckler, D.S. & Jester, J.V. (2007) Application of second harmonic imaging microscopy to assess structural changes in optic nerve head structure *ex vivo*. *J. Biomed. Opt.* **12**, 024029.

Bueno, J.M. & Vohnsen, B. (2005) Polarimetric high-resolution confocal scanning laser ophthalmoscope. *Vision Res.* **45**, 3526–3534.

Chu, S.-W., Liu, T.-M., Sun, C.-K., Lin, C.-Y. & Tsai, H.-J. (2003) Real-time second-harmonic-generation microscopy based on a 2-GHz repetition rate Ti:sapphire laser. *Opt. Express* **11**, 933–938.

Fernández, E.J., Iglesias, I. & Artal, P. (2001) Closed-loop adaptive optics in the human eye. *Opt. Lett.* **26**, 746–748.

Franze, K., Grosche, J., Skatchkov, S.N. *et al.* (2007) Müller cells are living optical fibers in the vertebrate retina. *PNAS* **104**, 8287–8292.

Freund, I. & Deutsch, M. (1986) Second-harmonic microscopy of biological tissue. *Opt. Lett.* **11**, 94–96.

Han, M., Zickler, L., Giese, G., Walther, M. Loesel, F.H. & Bille, J.F. (2004) Second-harmonic imaging of cornea after intrastromal femtosecond laser ablation. *J. Biomed. Opt.* **9**, 760–766.

Han, M., Giese, G. & Bille, J.F. (2005) Second harmonic generation imaging of collagen fibrils in cornea and sclera. *Opt. Express* **13**, 5791–5797.

Hermann, B., Fernández, E.J., Unterhuber, A. *et al.* (2004) Adaptive-optics ultrahigh-resolution optical coherence tomography. *Opt. Lett.* **29**, 2142–2144.

Hochheimer, B.F. (1982) Second harmonic light generation in the rabbit cornea. *Appl. Opt.* **21**, 1516–1518.

Labarthet, F.L. & Shen, Y.R. (2003) Nonlinear optical microscopy. *Optical imaging and microscopy* (ed. by F.-J. Kao and P. Török), chapter 7. Springer Verlag, Berlin.

Moreaux, L., Sandre, O., Blanchard-Desce, M. & Mertz, J. (2000) Membrane imaging by simultaneous second-harmonic generation and two-photon microscopy. *Opt. Lett.* **25**, 320–322.

Morishige, N., Wahlert, A.J., Cristina Kenney, M. *et al.* (2007) Second-harmonic imaging microscopy of normal human and keratoconus cornea." *Inv. Ophthalmol. Vis. Sci.* **48**, 1087–1094.

Palero, J.A., de Bruijn, H.S., Van Der Ploeg-van den Heuvel, A., Sterenborg, H.J.C.M. & Gerritsen, H.C. (2006) In vivo nonlinear spectral imaging in mouse skin. *Opt. Express* **14**, 4395–4402.

Qu, Y. & Singh, S. (1995) Measurements of photon statistics in second-harmonic generation. *Phys. Rev. A* **51**, 2530–2536.

Smith, T.B. (2007) Modeling corneal transparency. *Am. J. Phys.* **75**, 588–596.

Stoller, P., Celliers, P.M., Reiser, K.M. & Rubenchik, A.M. (2003) Quantitative second-harmonic generation microscopy in collagen. *Appl. Opt.* **42**, 5209–5219.

Sun, H., Han, M., Niemz, M.H. & Bille, J.F. (2007) Femtosecond laser corneal ablation threshold: dependence on tissue depth and laser pulse width. *Lasers Surg. Med.* **39**, 654–658.

Svoboda, K.K.H., Petroll, M.W. & Jester, J.V. (2007) Second harmonic signal analysis of whole embryonic avian corneas. *Microsc. Microanal.* **13**, 1550–1551.

Tan, H.-Y., Teng, S.-W., Lo, W., Lin, W.-C., Lin, S.-J., Jee, S.-H. & Dong, C.-Y. (2005) Characterizing the thermally induced structural changes to intact porcine eye, part 1: second harmonic generation imaging of cornea stroma. *J. Biomed. Opt.* **10**, 054019.

Teng, S.-W., Tan, H.-Y., Peng, J.-L. *et al.* (2006) Multiphoton autofluorescence and second-harmonic generation imaging of the ex vivo porcine eye. *Inv. Ophthalmol. Vis. Sci.* **47**, 1216–1224.

Vargas-Martín, F., Prieto, P.M. & Artal, P. (1998) Correction of the aberrations in the human eye with a liquid crystal spatial light modulator: limits to the performance. *J. Opt. Soc. Am. A* **15**, 2552–2562.

Vohnsen, B. & Artal, P. (2007) Multiphoton imaging of cornea and retinal tissues. *Invest. Ophthalmol. Vis. Sci.* **48**, E-Abstract4257.

Vohnsen, B. & Bozhevolnyi, S.I. (2001) Near- and far-field second-harmonic imaging of quasi-phase-matching crystals. *J. Microsc. (Oxford)* **202**, 244–249.

Vohnsen, B., Bozhevolnyi, S.I., Pedersen, K., Erland, J., Jensen, J.R. & Hvam, J.M. (2001) Second-harmonic scanning-optical microscopy of semiconductor quantum dots. *Opt. Commun.* **189**, 305–311.

Vohnsen, B., Iglesias, I. & Artal, P. (2005a) Directional light scanning laser ophthalmoscope. *J. Opt. Soc. Am. A* **22**, 2606–2612.

Vohnsen, B., Iglesias, I. & Artal, P. (2005b) Guided light and diffraction model of human-eye photoreceptors. *J. Opt. Soc. Am. A* **22**, 2318–2328.

Wang, B.-G. & Halbhuber, K.-J. (2006) Corneal multiphoton microscopy and intratissue optical nanosurgery by nanojoule femtosecond near-infrared pulsed lasers. *Ann. Anat.* **188**, 395–409.

Yeh, A.T., Nassif, N., Zoumi, A. & Tromberg, B.J. (2002) Selective corneal imaging using combined second-harmonic generation and two-photon excited fluorescence. *Opt. Lett.* **27**, 2082–2084.

Zayats, A.V. & Smolyaninov, I.I. (2004) Near-field second-harmonic generation. *Phil. Trans. – London A* **362**, 843–860.

Zipfel, W.R, Williams, R.M. & Webb, W.W. (2003) Nonlinear magic: multiphoton microscopy in the biosciences. *Nature Biotech.* **21**, 1369–1377.

